

## Herschel and the TeraHertz sky

Laurent Pagani<sup>a</sup>, Fabrice Herpin<sup>b</sup>, Maryvonne Gerin<sup>c</sup>, Pierre J. Encrenaz<sup>d</sup>

<sup>a</sup>LERMA, UMR8112 du CNRS, Observatoire de Paris, 61, Av. de l'Observatoire, 75014 Paris

<sup>b</sup>Université de Bordeaux, CNRS, UMR 5804, Laboratoire d'Astrophysique de Bordeaux, Observatoire Aquitain des Sciences de l'Univers, 2 rue de l'Observatoire, B.P.89, 33 271 Floirac Cedex, France

<sup>c</sup>LERMA, UMR8112 du CNRS, Ecole Normale Supérieure, 24 rue Lhomond, 75231 Paris Cedex 05, France

<sup>d</sup>LERMA, UMR8112 du CNRS, Observatoire de Paris, 61, Av. de l'Observatoire, 75014 Paris

---

### Abstract

Herschel is a spatial submillimetre observatory with spectroscopic and imaging capabilities covering the range from 55 to 671  $\mu\text{m}$  partly explored for the first time here. With a primary mirror of 3.5 m, it is presently the largest telescope launched. Its primary targets are the cold dust, the light hydrides, with a special focus on  $\text{H}_2\text{O}$ , and a few species of high interest like  $\text{C}^+$  and  $\text{O}_2$  in both our Galaxy and other galaxies. Its main focus is on star formation in all its possible aspects including cosmological metal enrichment evolution, statistics on prestellar cores or chemistry of protostar outflow terminal shocks to name only a few. We will describe the telescope and its three instruments, a selection of general results and we will focus on one typical case in greater detail, the observation of water in massive star forming regions. Herschel was launched in May 2009 and should last 3.5 years. *To cite this article: L. Pagani, F. Herpin, M. Gerin, & P.J. Encrenaz, C. R. Physique 13 (2012).*

### Résumé

**Herschel explore les cioux TéraHertz** Herschel est un observatoire submillimétrique spatial avec des capacités en imagerie et en spectroscopie couvrant de 55 à 671  $\mu\text{m}$ , une région en partie jamais explorée à ce jour. Avec un miroir primaire de 3,5 m, c'est le plus grand télescope mis en orbite à ce jour. Ses objets d'étude principaux sont la poussière froide, les hydrides légers avec en particulier  $\text{H}_2\text{O}$  et quelques espèces très intéressantes comme  $\text{C}^+$  et  $\text{O}_2$ , dans notre Galaxie et dans d'autres. Son premier centre d'intérêt est la formation des étoiles dans tous ses aspects y compris l'évolution cosmologique de l'enrichissement en métaux, la statistique des cœurs préstellaires ou la chimie dans les chocs terminaux des flots bipolaires des protoétoiles parmi tant d'autres. Nous décrivons le télescope et ses trois instruments, présentons une sélection de résultats généraux et nous exposons plus en détail un cas représentatif : l'observation de l'eau dans des régions de formation d'étoiles massives. Herschel a été lancé en mai 2009 et devrait fonctionner 3 ans et demi. *Pour citer cet article : L. Pagani, F. Herpin, M. Gerin, & P.J. Encrenaz, C. R. Physique 13 (2012).*

*Key words:* Telescopes ;ISM : molecules ; ISM : abundances ; Stars : formation ; Stars : protostars ; Stars : early-type ;  
Line : profiles

*Mots-clés :* Téléscopes ; MIS : molécules ; MIS : abondances ; Etoiles : formation ; Etoiles : proto-étoiles ; Etoiles : étoiles  
jeunes ; Raies : profils

## 1. Introduction

With Herschel, the last window of the electromagnetic spectrum opens up to our eyes[1]. Herschel, named FIRST until 2000 before changing name to celebrate the bicentenary of the discovery of infrared radiation [IR] by Sir W. Herschel is a project which started in 1982 when no IR satellite had been launched yet. The handful of IR spatial observatories which appeared in between had in common a small primary mirror (60 to 80 cm) actively cooled to 4 K to push their sensitivity to its best. They also covered mostly the mid and far IR domains, between 3 and 200  $\mu\text{m}$ . This corresponds to objects warmer than 15 K thereby excluding most of the dust, too cold ( $\sim 10$  K) to be detected with these observatories. These instruments had also limited spectral resolution due to the compulsory use of optical devices (Fourier transform spectrometres, Fabry-Pérot,...). Herschel was conceived from the start as a totally different observatory: a much larger (3.5 m) but passively cooled primary mirror with a far IR and a submm cameras with limited spectral resolution and a heterodyne spectrometre with a single pixel but high spectral resolution ( $\sim 10^7$ ). As a spatial heterodyne spectrometre, Herschel was preceded by two small spacecrafts, SWAS [2] and Odin [3] with limited capabilities (low sensitivity, low resolution, covering lines in the range 480-580 GHz only plus a 119 GHz O<sub>2</sub> channel for Odin). Herschel was launched the 14th of May 2009 together with Planck [4]. In Sect. 2, we present its most important technical characteristics, in Sect. 3, an overview of its first results with a particular focus on the study of water in high-mass star forming regions in Sect. 4.

## 2. The space observatory

The observatory is equipped with a dewar that contained 2367 litres of liquid Helium at launch. Positioned at the 2<sup>nd</sup> Lagrangian point, 1.5 Mkm from Earth, it should last about 3.5 years. The primary mirror has a useful diameter of 3.28 m with a surface accuracy better than 6  $\mu\text{m}$ . It is passively cooled to 85 K. The total weight of the spacecraft was 3.4 tons at launch, including 315 kg for the mirror, 426 kg for the instruments and 335 kg of He. The payload is made of 3 instruments, 2 bolometric cameras PACS and SPIRE and 1 heterodyne receiver, HIFI, which we detail now.

### 2.1. HIFI

HIFI, Heterodyne Instrument for the Far Infrared, was built by a large consortium of European and American laboratories[5]. It is made of 5 channels, 160 GHz wide each, covering the range 480-1250 GHz with Superconductor-Insulator-Superconductor [SIS] technology and 2 channels covering the range 1410 to 1910 GHz with Hot Electron Bolometre [HEB] technology. Only one channel (composed of two orthogonal linearly polarized mixers) can be connected at a time to the set of backends. These backends include a wideband low resolution Acousto-Optical spectrometre [AOS] (4 AOS of 1 GHz each with  $\sim 1.1$  MHz resolution per polarisation) and a versatile autocorrelator with a programmable resolution between 0.125 and 1 MHz but a narrower bandwidth (which depends on the resolution). The two spectrometres work in parallel, the autocorrelator acting as a zoom on any parts of the 4 GHz total bandwidth, being able to be split up in up to 4 independent subwindows. The two polarisations are considered as an internal redundancy and there is no spare receiver. Their outputs can be averaged to gain  $\sqrt{2}$  in sensitivity. The spatial resolution is limited by the primary mirror diffraction (modulo the illumination function) and

---

*Email addresses:* laurent.pagani@obspm.fr (Laurent Pagani), herpin@obs.u-bordeaux1.fr (Fabrice Herpin), maryvonne.gerin@ens.fr (Maryvonne Gerin), pierre.encrenaz@obspm.fr (Pierre J. Encrenaz).

varies from  $48''$  at 500 GHz to  $16''$  at 1.5 THz, giving resolutions comparable to the large ground-based mm telescopes. The main beam efficiency is high for an on-axis Cassegrain ( $\sim 0.7$ , [6]). Dual Beam Switch, Frequency Switch and On-The-Fly modes are offered.

## 2.2. SPIRE

SPIRE (Spectral and Photometric Imaging REceiver) is composed of a submillimetre camera and a low resolution spectrometre [7]. The camera is subdivided in 3 pixel planes centred at 250, 350, and 500  $\mu\text{m}$  in photometre mode ( $\lambda/\Delta\lambda \approx 3$ ), observing simultaneously and covering a  $4' \times 8'$  field of view. The number of pixels is 139, 88 and 43 respectively. It must be noted that each pixel is an independent bolometre with its individual coupling to the sky via a conic horn. In this type of receiver, pixels on the sky cannot be closer than twice their size and the camera must be moved at least three times to fill in the gaps. In general, this is no limitation as SPIRE is meant to map large portions of the sky by sweeping several times across the desired field. It is interesting to remark that the two channels centred at 350 and 500  $\mu\text{m}$  are very close to the two highest frequency bolometres on-board Planck (at 545 and 857 GHz, equivalent to 550 and 355  $\mu\text{m}$ ). This should allow interesting synergies between the two instruments.

The spectrometre has also imaging capabilities and covers a circular field of  $2.6'$  in diameter. It is a Fourier transform spectrometre and its resolution is ranging between  $\lambda/\Delta\lambda \approx 370$  at long wavelengths and  $\lambda/\Delta\lambda \approx 1300$  at short wavelengths. The camera behind is split in two units, one of 37 pixels covering the range from 194 to 324  $\mu\text{m}$ , and one of 19 pixels covering the range from 316 to 671  $\mu\text{m}$ .

All bolometres are cooled down to 0.3 K from the 2 K stage to which is appended a Helium-3 ( $^3\text{He}$ ) cryocooler. This cryocooler has no mechanical part and works in a close-loop cycle based on evaporation of a liquid. These coolers last 2 days before all the liquid  $^3\text{He}$  is evaporated. The coolers are then recycled (by reliquefaction of the  $^3\text{He}$  gas). Though very cold, they do not match the extreme cooling performance on board Planck which reach 0.1 K (space record) but based on a different principle ( $^3\text{He}$  dilution in  $^4\text{He}$  liquid).

## 2.3. PACS

From the science point of view, PACS (Photodetector Array Camera and spectrometre)[8] is the least original instrument because it covers wavelengths already explored with several of the previous IR satellites. It is still very interesting though because it has gained from technical improvements over its predecessors (more pixels, higher sensitivity) but mostly because thanks to the large primary mirror, it has a much better spatial resolution (factor 4 compared to ISO, [9]) which is always interesting, in particular in extragalactic work to push the confusion limit further down. Like SPIRE, it offers three photometric cameras centred on 70, 100 and 160  $\mu\text{m}$  but the three cameras cannot operate simultaneously because there are only two bolometre matrices, one with 2048 pixels which covers the two short wavelength bands with the help of pass-band filters to select one or the other, one with 512 pixels for the long wavelengths. Thus one can observe simultaneously at 70 and 160  $\mu\text{m}$  or at 100 and 160  $\mu\text{m}$ . The field of view is smaller than for SPIRE ( $1.75' \times 3.5'$ ) but here the pixels touch each other on the sky and it is not necessary to shift the receiver to build an image. The pixel size on the sky is  $3.2''$  at short wavelength and  $6.4''$  at long wavelength. These bolometre matrices were never built before at these wavelengths and represent a technical achievement. The spectrometre is a blazed grating of the Littrow type which allows for a very compact design by using the same lens as input to and output from the grating. Its range is comparable to the long wavelength spectrometre of ISO (ISO/LWS) [9] though with a lower resolution ( $\lambda/\Delta\lambda \approx 1000-4000$ ) but with a higher sensitivity. The spectro-imager contains 25 pixels positioned approximatively on a square with a total size of  $47'' \times 47''$ .

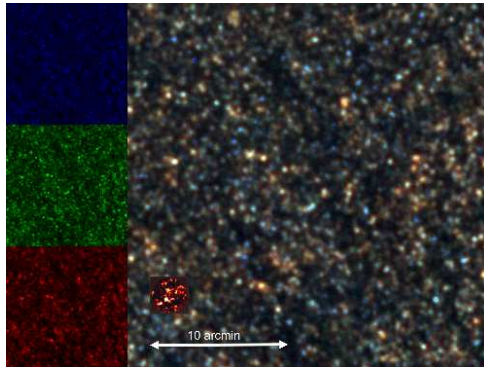


Figure 1. Deep images of remote galaxies in the early universe obtained with the SPIRE photometre. The three channels at 250, 350 and 550  $\mu\text{m}$  are coded with blue, green and red colors respectively [10].

There exists a common mode using PACS and SPIRE in parallel, covering therefore all 5 bands from 100 to 500  $\mu\text{m}$  at once. This is very well suited to map cold dust as the cold dust emission peak is always inside this wavelength range. This has been extensively used to map hundreds of square degrees in our Galaxy, delivering astounding images of cold dust filaments with many prestellar cores and protostars aligned inside them. Spectroscopy is not delivering such spectacular images but the physics behind is powerful to help us understand the star formation process.

### 3. A selection of scientific results

We present hereunder a small selection of interesting scientific results taken among the many results published in the two A&A special issues (vol. 518 and 521, 2010) and in subsequent individual publications.

#### 3.1. Formation of galaxies

The infrared and sub-millimetre wavelength range is particularly well suited for studying the first phases of galaxy formation for two reasons : *i*) at the large redshift of the first galaxies ( $z > 5$ ), the main spectral features are shifted to the near and mid infrared spectral ranges ; *ii*), due to the presence of dust the most active burst of star formation mostly radiate in the far infrared spectral range. In the rest wavelength reference frame, this far infrared radiation is typically maximum around 100  $\mu\text{m}$  and steeply decreases as a modified blackbody  $S_\nu \sim \nu^{3.5}$  for sub-millimetre wavelengths. Depending on the source redshift, it is redshifted to sub-millimetre wavelengths, ranging between 200 and 1000  $\mu\text{m}$  for redshifts 1 to 10. Therefore the observed fluxes of distant galaxies do not strongly depend on their redshift as the dimming in distance is compensated by the larger emission at shorter wavelengths. This effect is known as the “negative k-correction”. The first deep images taken with the SPIRE photometre are excellent examples of this effect : the image background is studded with numerous point sources, each of them being one distant galaxy (or a group of them since they are so many that several distinct objects can contribute to the same sub-millimetre source). These deep images allow robust statistical studies of the population of sub-millimetre galaxies in the early universe. They are also useful to select interesting targets for follow up studies at higher spatial resolution.

### 3.2. *Star formation*

The formation of stars and their subsequent impact on the interstellar medium is recognized as one of the main theme of today's astrophysics. With its versatile instruments, the Herschel Space Observatory is particularly well adapted to make progresses on star formation. The SPIRE and PACS photometres are producing wide field images of star forming regions with unprecedented quality, while the spectrometre give access to the gas dynamics over a broad range of spatial scales, revealing the interplay of infall motions associated with gravitational collapse, and large scale flows (see Sect. 4).

Thanks to the high sensitivity and large mapping capabilities, Herschel is providing better statistical information on the dense structures where stars form. It was already known that star form in the densest and coldest regions of molecular clouds, the so-called dense cores. The new Herschel results nicely confirm that the mass distribution of these dense cores is very similar to the mass distribution of forming stars (the so called Initial Mass Function or IMF), while the mass distribution of unbound structure presents a shallower slope. In addition, the dense regions are organized along a network of dense filaments, with the dense cores appearing as nodes along the filaments [11]. Only the densest filaments harbor dense cores and star formation. In more diffuse regions, the structure are not bound and the self similar structure is likely created by the magneto-hydrodynamic (MHD) turbulence [12].

### 3.3. *The Molecular Universe*

Thanks to its wide wavelength coverage and the access to a poorly explored region of the electromagnetic spectrum, Herschel has discovered many new spectral features, including several detections of new molecules. Most of them belong to the class of hydrides combining one or several hydrogen atoms with a heavy element, as the neutral molecules  $\text{H}_2\text{O}$ ,  $\text{NH}_3$ ,  $\text{HF}$ , the  $\text{CH}$ ,  $\text{NH}$  and  $\text{NH}_2$  radicals, or the  $\text{CH}^+$ ,  $\text{OH}^+$ ,  $\text{H}_2\text{O}^+$ ,  $\text{H}_2\text{Cl}^+$  reactive ions. Isotopologues bearing  $^{18}\text{O}$ ,  $^{13}\text{C}$  or  $\text{D}$  are also within reach for Herschel as shown in Fig 2 [13,15,16]. Spectral line surveys have been performed over the full HIFI wavelength coverage, from 480 to 1250 GHz and from 1430 to 1900 GHz, two orders of magnitude improvement in the spectral coverage and observing speed compared to previous spectral surveys [17,18]. Two molecules have deserved a special attention in the Herschel programmes : water vapor and molecular oxygen, because they are very difficult to observe from the ground. In both cases, Herschel results have been amazing. Some results of water vapor are presented in Sect. 4. As for  $\text{O}_2$ , Goldsmith et al. and Liseau et al. ([19,?]) present good evidences for the presence of molecular oxygen in different regions, with an abundance relative to  $\text{H}_2$  of the order of  $10^{-7}$ , not easily explained by state of the art chemical models.

### 3.4. *Stellar evolution*

The complete spectral coverage of the Herschel spectrometres, from 50 to 700  $\mu\text{m}$  has lead to the discovery of many interesting spectral features in the spectra of evolved stars, leading to a revised picture of the late stage of stellar evolution. For instance water vapor has been detected in the extreme carbon star IRC+10216 by the SWAS and ODIN satellites, but with their higher sensitivity and spectral resolution, the Herschel data allow not only to confirm the detection, but also provide a convincing explanation of the presence of water vapor in this star : water is formed in the very inner regions close to the photosphere where a small amount of Oxygen can be locked into water [21]. Other important results include the detection of Hydrogen Chloride ( $\text{HCl}$ ) and ammonia ( $\text{NH}_3$ ) in IRC+10216 and the wealth of water lines in the far infrared spectrum of the O-rich star V $\gamma$ CMa [22].

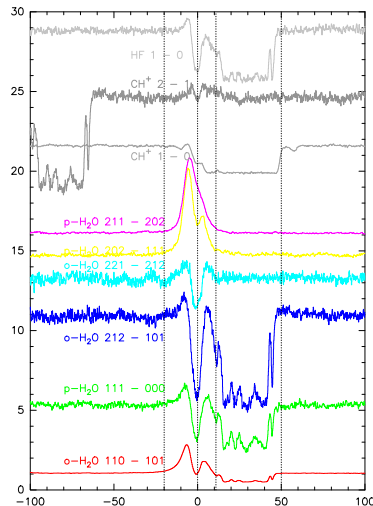


Figure 2. Examples of hydride spectra obtained towards the massive star forming region G10.6–0.4. The line of sight intersects several diffuse interstellar clouds that show up as absorption features in the velocity range  $\sim 10 - -50 \text{ km s}^{-1}$ , while the line profiles from the background source combine emission and absorption ( $-10$  to  $10 \text{ km s}^{-1}$ ).

### 3.5. Planet formation and Solar system

Proto-planetary and debris disks are primary targets for Herschel as they represent previous stages of the solar system evolution, and the birth places of planets. Proto-planetary disks are typically detected by their excess emission over the stellar photosphere at IR wavelength, or as deep extinction regions, in young protostars (less than 1 Myr). The gas dynamics as probed by CO and other molecular lines show Keplerian rotation and allow precise determination of the stellar masses. Debris disks are detected around stars up to  $\sim 100$  Myrs. They harbor mainly solid particles resulting from the erosion of larger bodies (planetesimal or even planets) with very little gas remaining. Both categories have been targeted by Herschel, leading to surprising results :

- The fine structure line of atomic oxygen is one of the strongest spectral feature [23]
- Water lines are quite prominent in disks illuminated by A stars but extremely weak around TTauri (solar type) stars [24]. This variation is difficult to understand with state of the art models that include water freeze-out and desorption.
- Numerous CO lines up to energy levels above 1000 K are detected in disk atmospheres.
- Several emission lines from the extremely reactive ion  $\text{CH}^+$  have also been detected, showing that an active chemistry is taking place in the disk atmospheres [25].

Comets carry key information on the origin of the solar system, since these objects are less processed than the massive planets. These icy objects are primarily made of water ice, mixed with refractory material (dust grains) and traces of other frozen volatiles. Herschel observations allow the direct observation of the main molecular ejecta such as  $\text{H}_2\text{O}$  and its isotopologues ( $\text{H}_2^{18}\text{O}$  and  $\text{HDO}$ , before they are processed and destroyed by the solar radiation. The isotopic ratio  $\text{HDO}/\text{H}_2\text{O}$  has been measured in the Jupiter family comet Comet 103P/Hartley 2 [26] and found similar to deuterium abundance in the Earth’s oceans, suggesting that such comets could have provided the Earth’s water. This is the first measurement in a comet of this family with short periods. Previous measurements in Oort family comets provided larger  $\text{HDO}/\text{H}_2\text{O}$  value, clearly not compatible with the hypothesis of comets as the source of the Earth’s oceans. More  $\text{HDO}$  observations are planned to improve the statistics.

#### 4. A detailed result: water in massive-star forming regions

In the deeply embedded phase of star formation, it is often only possible to trace the dynamics of gas in a young stellar object (YSO) through resolved emission-line profiles. The various dynamical processes include infall from the surrounding envelope towards the central protostar, molecular outflows, and strong turbulence. One of the goals of Herschel and of its spectrometre HIFI is to probe these processes and determine the abundance of the chemical species as a function of evolution.

##### 4.1. *Water in the Universe*

Water is a common species in the Universe (it is the third most abundant molecular species, mostly in gas phase), but is quasi-unobservable from the ground because of our own atmosphere. Only space observations can allow us to study the water emission and hence to determine its quantity and chemistry. Because of its importance for life, its role in the evolution of stars, and its sensitivity to dynamical, thermal and chemical processes, water study is one of the main drivers of Herschel, and more especially of the HIFI spectrometre [5] on-board. Thanks to Herschel, for the first time a large fraction of the energy ladder of water is observable.

To make water molecules, hydrogen (H) and oxygen (O) atoms are needed. But the Big Bang created only two elements: hydrogen (75 %) and helium (25%). The other chemical elements (oxygen, carbon, iron..) have been produced later from the nuclear transmutation of H and He within the first stars, before our Solar system was created. The production of all these elements and even heavier ones goes on in mainly two types of stars:

- Solar-type stars which produce O, N, C;
- massive stars (more than 8 times the Sun mass) which produce Si, Ne, C, O, and Fe.

But water is (quasi-) unobservable from the ground because of our own atmosphere. Only space observations can allow us to study the water emission and hence to determine its quantity and chemistry.

##### 4.2. *High mass star formation problematic*

The OB stars are the main contributors to the evolution and energy budget of galaxies. These massive stars, even rare (only a few % of the total), are essential for the life and matter cycle in the Universe. The heavy elements such as O, Si, Ne, C or Fe, produced in these stars, are later ejected and incorporated in the diffuse interstellar medium, then transformed into molecular material in the dense clouds, and will be eventually re-used for another cycle, possibly to create life. Their formation, however, has not been understood yet and the classical scheme for low-mass star formation cannot be applied as such to OB stars. Indeed, young OB stars and protostars strongly interact with the surrounding massive clouds and cores, leading to a complex and still not clearly defined sequence of objects from pre-stellar cores, that are often believed to be hosted in the so-called IR dark clouds, to high-mass protostellar objects (HMPOs), to hot molecular cores (HMC) and Ultra Compact HII regions [27]. The most problematic issue in the massive star formation process is to understand how the accretion of matter overcomes radiative pressure. Two theoretical scenarios try to solve this issue: a turbulent core model with a monolithic collapse scenario [28],[29], and a (highly dynamical) competitive accretion model involving the formation of a cluster [30]. In ionized HII regions, triggered star formation could also take place [31]. In the deeply embedded phase of star formation, it is often only possible to trace the dynamics of gas in a young stellar object through resolved emission-line profiles.

### 4.3. The WISH Key-Program

The WISH GT-KP (Water In Star forming regions with Herschel, PI: E. van Dishoeck, [32]) aims at probing the stellar formation through water observations with HIFI and PACS towards a large sample of low-, intermediate- and high-mass protostellar objects and circumstellar disks. The large variations of water abundance (e.g. evaporation from dust grains for  $T > 100$  K) depending on the physical conditions allow to test different regions, and, hence, to characterize different evolutionary stages. Also, water is a very good probe of gas flows (infall, outflow). But maybe more important, water plays a crucial role in the energy balance and, as an efficient cooling agent, could help to understand how massive stars can form. Finally, water molecules are the main oxygen reservoir.

### 4.4. Results

The study of the high-mass protostar formation represents a large fraction of the WISH KP. This part is led by F. Herpin (LAB-France), F. van der Tak (SRON- Netherlands) and F. Wyrowski (MPIfR-Germany). It consists of HIFI pointed observations of 14 water lines, including rare isotopic lines ( $\text{H}_2^{18}\text{O}$ ,  $\text{H}_2^{17}\text{O}$ ) in 19 sources (plus deep  $\text{H}_2\text{O } 1_{10} - 1_{01}$  observation of four infrared-dark cloud cores) at different evolutionary stages (mid-IR-quiet and mid-IR-bright massive dense cores, hot molecular cores and UCHII regions). Maps of water emission with HIFI ( $1_{10} - 1_{01}$ ,  $2_{02} - 1_{11}$ ,  $1_{11} - 0_{00}$ ) and PACS maps in 4 lines of 6 proto-clusters are also performed. The goal is to determine the abundance and distribution of water in the envelopes, massive outflows, and to precise the filling, cooling and chemistry of intra-cluster gas. The observations include chemically related species (O, OH,  $\text{H}_3\text{O}^+$ ), radiation diagnostics of UV and X-rays, and a few key high-J CO lines too. The interpretation of the data is made through the line profile analysis and a line modelling Whitney-Robitaille (hereafter WR) code [33,34,35] for the continuum and RATRAN [36] for the lines.

A first look to the water line profiles towards objects with different mass shows that water lines are stronger and more complex in high-mass protostellar objects (see Fig.3). The DR21(Main), in Cygnus X ( $L=45000 L_{\odot}$ ,  $d=1.7$  kpc) region, a relatively evolved object, was observed by the HSO [37] in the  $^{13}\text{CO } 10-9$  and  $\text{H}_2\text{O } 1_{11} - 0_{00}$  (1113 GHz) lines. The profiles exhibit different components coming from the outflow, the protostellar envelope itself, and a foreground cloud. The high water abundance ( $7 \cdot 10^{-7}$ ) in the warm outflow is probably due to the evaporation of water-rich icy grain mantles, while the  $\text{H}_2\text{O}$  abundance is kept down by freeze-out in the dense core ( $1.6 \cdot 10^{-10}$ ) and by photodissociation in the foreground cloud ( $4 \cdot 10^{-9}$ ).

Marseille et al. (2010) [41] published the first comparison of water spectra ( $\text{H}_2\text{O}$  and  $\text{H}_2^{18}\text{O } 1_{11} - 0_{00}$ ,  $\text{H}_2\text{O } 2_{02} - 1_{11}$ , see Fig.4) obtained in W43-MM1 (mid-IR quiet HMPO), W33A (mid-IR bright HMPO), G31.41+0.31, and G29.96-0.02 (HMC). A first estimate of the water abundance has been made for all these objects. The higher abundance ( $> 10^{-8}$ ) derived for G31.41+0.31 and W43-MM1 is not clearly linked to luminosity, mass and temperature or assumed evolutionary stage of the source.

The mid-IR bright massive dense core W3-IRS5 (Perseus region,  $d=2.0$  kpc) was studied by [38]. Several water lines have been observed and modeled. Emission in the rare isotopologue lines is only reproduced in the models by including a jump in the water abundance in the inner envelope. The emission in the rare species comes from the inner envelope where the water abundance is greatly enhanced (evaporation from dust grains). Emission from this region could be the expected contribution from the passively radiatively heated inner envelope. The signature of outflow (high-velocity emission of  $33-40 \text{ km s}^{-1}$ ) is seen, but no infall is observed. Profiles reveal absorption from the cold molecular cloud ( $T \leq 10$  K) in which the proto-stellar envelope is embedded. From the model interpretation, we conclude that the water emission is coming from the 2 sources first observed by Rodon et al. (2008) [42]. The water abundance is  $10^{-4}$  in



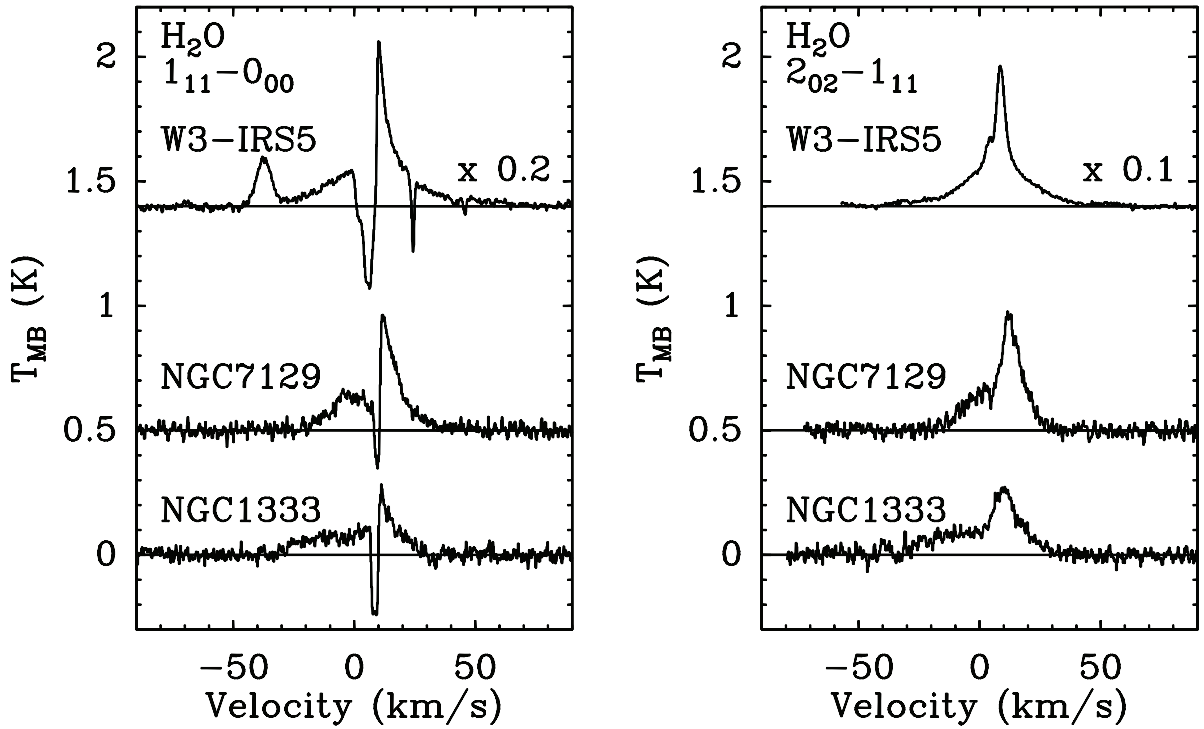


Figure 3. HIFI spectra of the para- $\text{H}_2\text{O}$   $1_{11} - 0_{00}$  1113 GHz (left) and  $2_{02} - 1_{11}$  988 GHz (right) lines. From top to bottom: the high-mass YSO W3 IRS5 ( $L = 1.5 \times 10^5 L_{\odot}$ ,  $d = 2.0$  kpc) [38], the intermediate-mass YSO NGC 7129 FIRS2 ( $430 L_{\odot}$ , 1260pc) [39], and the low-mass YSO NGC 1333 IRAS2A ( $20 L_{\odot}$ , 235 pc) [40].

the inner protostellar envelope ( $T > 100\text{K}$ ) while it is  $10^{-8}$ – $10^{-9}$  in the outer envelope (see Fig.5).

Finally, a large study of the chemistry has been made by Benz et al. (2010) [43] for W3-IRS5 and Bruderer et al. (2010) [44] for AFGL2591 within the WISH KP. Through the observations of various hydrides, a radiation diagnostic in the system protostar-disk-outflow is possible. Actually, hydrides are produced at high temperatures via reactions with atomic ions within strong UV or X fields. The following species have been detected: OH, CH ( $2 \times 10^{-8}$  in AFGL2591), NH ( $10^{-9}$ ), SH,  $\text{OH}^+$  ( $3 \times 10^{-10}$ ),  $\text{CH}^+$  ( $10^{-8}$ ),  $\text{NH}^+$ ,  $\text{SH}^+$ ,  $\text{H}_2\text{O}$ ,  $\text{H}_2\text{O}^+$  ( $7 \times 10^{-10}$ ),  $\text{H}_3\text{O}^+$ . The first detection of  $\text{OH}^+$  and  $\text{H}_2\text{O}^+$  [45] reveals the gas phase path to produce water, and, hence, complete the water chemical puzzle. They conclude that FUV radiation from central protostar irradiates and heats the walls of the outflow cavity making the abundance of  $\text{CH}^+$ ,  $\text{OH}^+$  and  $\text{NH}^+$  to increase by several orders of magnitude in the walls of the outflow.

## Acknowledgements

The Herschel spacecraft was designed, built, tested, and launched under a contract to ESA managed by the Herschel/Planck Project team by an industrial consortium under the overall responsibility of the prime contractor Thales Alenia Space (Cannes), and including Astrium (Friedrichshafen) responsible for the payload module and for system testing at spacecraft level, Thales Alenia Space (Turin) responsible for the service module, and Astrium (Toulouse) responsible for the telescope, with in excess of a hundred subcontractors. HIFI has been designed and built by a consortium of institutes and university depart-

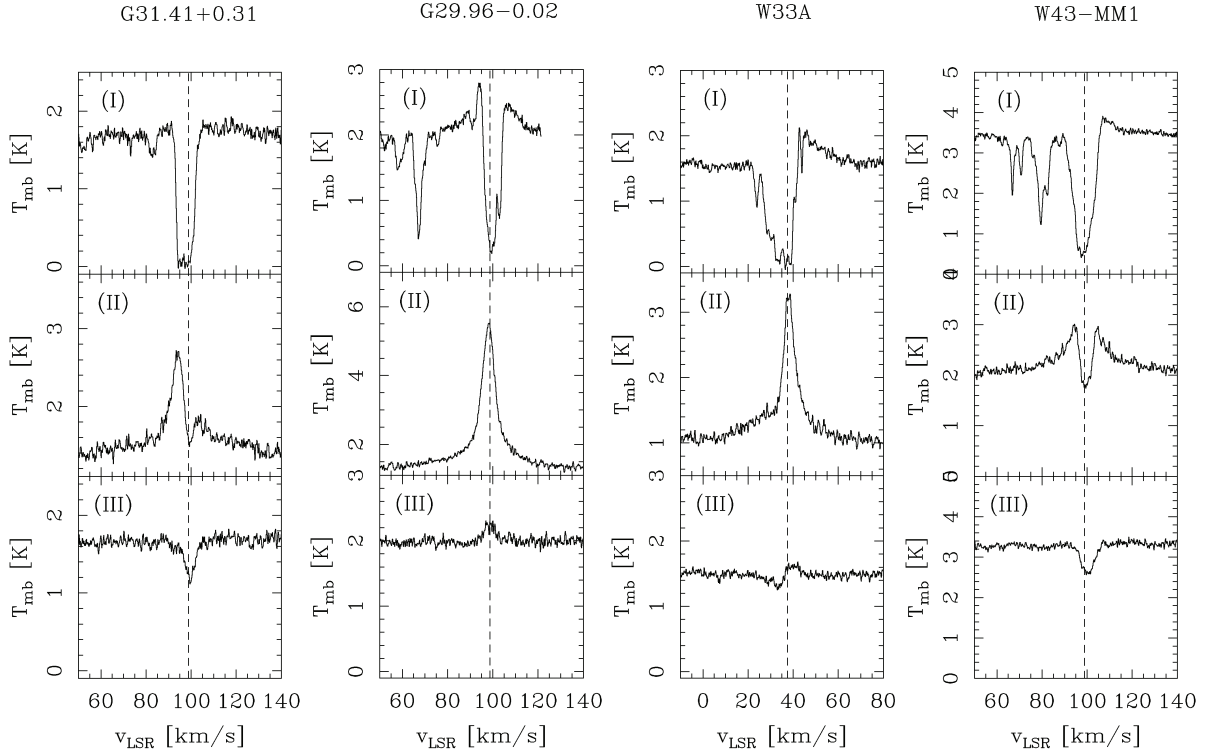


Figure 4. Herschel/HIFI spectra of the  $\text{H}_2\text{O } 1_{11} - 0_{00}$  (top),  $\text{H}_2\text{O } 2_{02} - 1_{11}$  (middle) and  $\text{H}_2^{18}\text{O } 1_{11} - 0_{00}$  (bottom) lines towards a few high-mass protostellar objects. Dashed lines drawn at VLSR [41].

ments from across Europe, Canada and the United States under the leadership of SRON Netherlands Institute for Space Research, Groningen, The Netherlands and with major contributions from Germany, France and the US. Consortium members are: Canada: CSA, U. Waterloo; France: CESR, LAB, LERMA, IRAM; Germany: KOSMA, MPIfR, MPS; Ireland, NUI Maynooth; Italy: ASI, IFSI-INAF, Osservatorio Astrofisico di Arcetri- INAF; Netherlands: SRON, TUD; Poland: CAMK, CBK; Spain: Observatorio Astronómico Nacional (IGN), Centro de Astrobiología (CSIC-INTA). Sweden: Chalmers University of Technology - MC2, RSS & GARD; Onsala Space Observatory; Swedish National Space Board, Stockholm University - Stockholm Observatory; Switzerland: ETH Zurich, FHNW; USA: Caltech, JPL, NHSC.

PACS has been developed by a consortium of institutes led by MPE (Germany) and including UVIE (Austria); KU Leuven, CSL, IMEC (Belgium); CEA, LAM (France); MPIA (Germany); INAF-IFSI/OAA/OAPD, LENS, SISSA (Italy); IAC (Spain). This development has been supported by the funding agencies BMVIT (Austria), ESA-PRODEX (Belgium), CEA/CNES (France), DLR (Germany), ASI/INAF (Italy), and CI-CYT/MCYT (Spain).

SPIRE has been developed by a consortium of institutes led by Cardiff University (UK) and including Univ. Lethbridge (Canada); NAOC (China); CEA, LAM (France); IFSI, Univ. Padua (Italy); IAC (Spain); Stockholm Observatory (Sweden); Imperial College London, RAL, UCL-MSSL, UKATC, Univ. Sussex (UK); and Caltech, JPL, NHSC, Univ. Colorado (USA). This development has been supported by national funding agencies: CSA (Canada); NAOC (China); CEA, CNES, CNRS (France); ASI (Italy); MCINN (Spain); SNSB (Sweden); STFC (UK); and NASA (USA).

HIPE is a joint development by the Herschel Science Ground Segment Consortium, consisting of ESA,

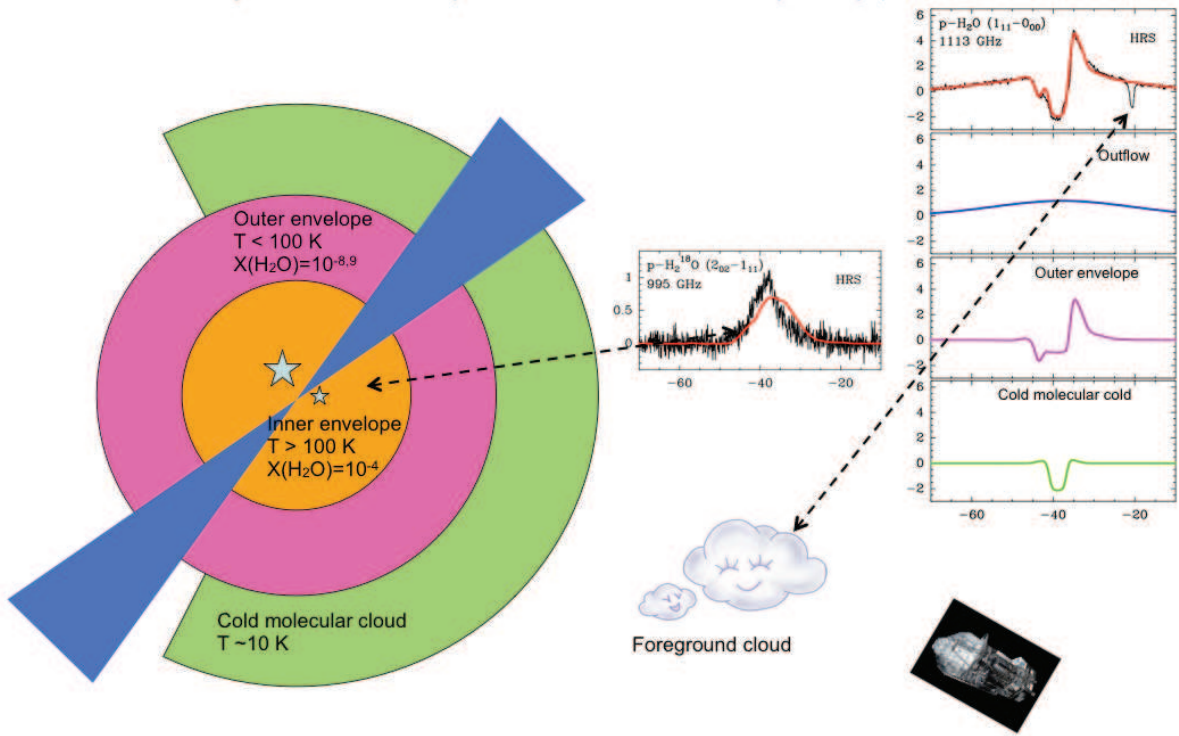


Figure 5. Schematic view of W3-IRS5 high-mass massive dense core and of the different components of the water line profiles [38].

the NASA Herschel Science Center, and the HIFI, PACS and SPIRE consortia.

The WISH program is made possible thanks to the HIFI guaranteed time. We also thank the French Space Agency CNES for financial support.

## References

- [1] Pilbratt, G. L., et al. 2010, A&A, 518, L1+
- [2] Melnick, G. J., et al. 2000, ApJL, 539, L77
- [3] Hjalmarson, Å., et al. 2003, A&A, 402, L39
- [4] Tauber, J. A., et al. 2010, A&A, 520, A1+
- [5] de Graauw, T., Helmich, F.P., Phillips, T. G., et al. 2010, A&A, 518, L6+
- [6] Teyssier, D., et al. 2010, in Twenty-First International Symposium on Space Terahertz Technology, 40–45
- [7] Griffin, M. J., et al. 2010, A&A, 518, L3+
- [8] Poglitsch, A., et al. 2010, A&A, 518, L2+
- [9] Kessler, M. F., et al. 1996, A&A, 315, L27
- [10] Oliver S.J., Wang L., Smith A.J., Altier I B. et al., 2010;A&A 518, L21
- [11] André P., Menšíkov A., Bontemps S., et al., 2010, A&A 518, L102.
- [12] Miville-Deschênes M.A., Martin P.G., Abergel A., 2010, A&A 518, L104.

- [13] Gerin M., de Luca M., Goicoechea J., et al., 2010, A&A 521, L21
- [14] Neufeld D.A., Sonnentrucker P., Phillips T.G. et al., 2010, A&A 518, L108.
- [15] Neufeld D.A., Goicoechea J.R., Sonnentrucker P. et al., 2010, A&A 521, L10.
- [16] Falgarone E., Godard B., Cernicharo J., et al., A&A 521, L15
- [17] Bergin E.A., Phillips T.G., Comito C., et al.? 2010, A&A 521, L20.
- [18] Ceccarelli C., Bacmann A., Boogert A., et al., 2010, A&A 521, L22.
- [19] Goldsmith P.F., Liseau R., Bell T., et al., 2011, ApJ 737, 96.
- [20] Liseau R., Goldsmith P.F., Larsson B., et al., 2011, A&A submitted.
- [21] Decin L., Agúndez M., Barlow M.J., 2010, Nature 467, 64.
- [22] Royer P., Decin L., Wesson R., et al., 2010, A&A 518, L145.
- [23] Mathews G.S., Dent W.R.F., Williams J.P., 2010, A&A 519, L127.
- [24] van Kempen T.A., Green J.D., Evans N.J., 2010, A&A 518, L128.
- [25] Thi W.F., Ménard F., Meeus G., et al, 2011, A&A 530, L2.
- [26] Lis D.C., Hartogh P., Bockelée-Morvan D. et al., 2011, Nature in press.
- [27] Beuther, H., Churchwell, E. B., McKee, C. F., & Tan, J. C. 2007, in Protostars and Planets V, ed. B. Reipurth, D. Jewitt, & K. Keil, 165180
- [28] McKee, C. F. & Tan, J. C. 2003, ApJ, 585, 850
- [29] Tan, J. C. & McKee, C. F. 2002, in Astronomical Society of the Pacific Conference Series, Vol. 267, Hot Star Workshop III: The Earliest Phases of Massive Star Birth, ed. P. Crowther, 267
- [30] Bonnell, I. A. & Bate, M. R. 2006, MNRAS, 370, 488
- [31] Deharveng, L., Zavagno, A., Schuller, F., et al. 2009, A&A, 496, 177
- [32] van Dishoeck E., Kristensen L., Benz A. et al. 2011, PASP, in press
- [33] Whitney, B. A., Wood, K., Bjorkman, J. E., & Wol, M. J. 2003, ApJ, 591, 1049
- [34] Robitaille, T. P., Whitney, B. A., Indebetouw, R., & Wood, K. 2007, ApJS, 169, 328
- [35] Robitaille, T. P., Whitney, B. A., Indebetouw, R., Wood, K., & Denzmore, P. 2006, ApJS, 167, 256
- [36] Hogerheijde, M.R., van der Tak, F.F.S. 2000, A&A, 362, 697
- [37] van der Tak, F.F.S., Marseille, M., Herpin, F. 2010, A&A, 518, 107
- [38] Chavarria, L., Herpin F., Jacq, T. et al. 2010, A&A 521, 37
- [39] Johnstone, D., Boonman, A.M.S., van Dishoeck, E.F. et al. 2010, A&A 521, 41
- [40] Kristensen, L., Visser, R., van Dishoeck, E.F. et al. 2010, A&A 521, 30
- [41] Marseille, D., van der Tak, F.F.S., Herpin, F. et al. 2010, A&A 521, 32
- [42] Rodon, J., Beuther, H., Megeath, T. et al. 2008, A&A, 490, 213
- [43] Benz, A., Bruderer, S., van Dishoeck, E. et al. 2010, A&A 521, 35
- [44] Bruderer, S., Benz, A., van Dishoeck, E. et al. 2010, A&A 521, 44
- [45] Wyrowski F., van der Tak F., Herpin F. et al. 2010, A&A 521, 34